Published in final edited form as:
J Immunol. 2010 July 1; 185(1): 660–669. doi:10.4049/jimmunol.1000471.

IL-13 induces esophageal remodeling and gene expression by an eosinophil-independent IL-13Rα2-inhibited pathway

Li Zuo[1], **Patricia C. Fulkerson**[2], **Fred D. Finkelman**[3], **Melissa Mingler**[1], **Christine A. Fischetti**[1], **Carine Blanchard**[1], and **Marc E. Rothenberg**[1,*]

[1]Division of Allergy and Immunology, Cincinnati Children's Hospital Medical Center, University of Cincinnati College of Medicine, 3333 Burnet Avenue, Cincinnati, OH 45229-3039, USA

[2]Departments of Molecular Genetics, Biochemistry & Microbiology, University of Cincinnati College of Medicine, 231 Bethesda Avenue, Cincinnati OH 45257-0524, USA

[3]Division of Immunology, Cincinnati Children's Hospital Medical Center, University of Cincinnati College of Medicine, 3333 Burnet Avenue, Cincinnati, OH 45229-3039, USA

Abstract

Eosinophilic esophagitis (EE) is an emerging disease associated with both food and respiratory allergy characterized by extensive esophageal tissue remodeling and abnormal esophageal gene expression including increased IL-13. We investigated the ability of increased airway IL-13 to induce EE-like changes. Mice that overexpress an IL-13 transgene in the lung (but not esophagus) accumulated esophageal IL-13 and developed prominent esophageal remodeling with epithelial hyperplasia, angiogenesis, collagen deposition and increased circumference. IL-13-induced marked changes in esophageal transcripts overlapped with the human EE esophageal transcriptome. IL-13-induced esophageal eosinophilia was eotaxin-1 (but not eotaxin-2) dependent but remodeling occurred independent of eosinophils, as demonstrated by studying eosinophil lineage-deficient IL-13 transgenic mice. IL-13-induced remodeling was significantly enhanced by IL-13Rα2 gene deletion, indicating an inhibitory effect of IL-13Rα2. In the murine system, there was partial overlap between IL-13-induced genes in the lung and esophagus, yet the transcriptomes were also divergent at the tissue level. In human esophagus, IL-13 levels correlated with the magnitude of the EE transcriptome. In conclusion, inducible airway expression of IL-13 results in an esophageal gene expression and extensive tissue remodeling pattern that resembles human EE. Notably, we have identified a pathway for inducing EE-like changes that is IL-13-driven, eosinophil-independent and suppressed by IL-13Rα2.

Esophageal eosinophilia occurs in a variety of disorders, including gastroesophageal reflux disease (GERD) and primary eosinophilic esophagitis (EE) (1, 2). EE is an emerging disorder presenting with GERD-like symptoms (vomiting, abdominal pain, failure to thrive, dysphagia, and food impaction) but does not respond to acid neutralization therapy. Rather, EE is largely mediated by oral- and aero-antigen-induced esophageal adaptive immunity and responds to anti-inflammatory agents (e.g. glucocorticoids) and food antigen elimination diets. There is extensive eosinophil accumulation in the proximal and distal esophagus and extensive tissue remodeling, including epithelial thickening and collagen deposition, even in pediatric individuals (3).

The etiology of EE is poorly understood, but allergy has been implicated. In fact, the majority of EE patients have evidence of food and aeroallergen hypersensitivity as defined

Correspondence should be addressed to M.E.R. (Rothenberg@cchmc.org), Phone: 513-636-7210, Fax: 513-636-3310.

by skin prick testing and in vitro lymphocyte responses (4). Previous studies have shown that repeated challenge of mice with intranasal Aspergillus fumigatus antigen induces lymphocyte dependent EE-changes, supporting the association between airway allergy and the development of EE (5). In addition, eosinophilic inflammation in the esophagus can be induced directly by intranasal or intratracheal human or murine IL-13 (6) and can be blocked by anti-human IL-13 antibody (6). Additionally, aeroallergen-induced EE is dependent upon IL-13, as assessed by failure of IL-13 gene-targeted mice to develop esophageal eosinophilia and epithelial hyperplasia (7). Based on these findings in mice, IL-13 may have a role in disease induction in humans. Indeed, IL-13 is overproduced in the esophagus of EE patients and is capable of inducing a gene expression profile in esophageal epithelial cells that partially overlaps with the esophageal transcriptome present in EE patients (8). The IL-13-induced epithelial cell-produced gene that is most overexpressed in the esophagus of EE patients is eotaxin-3, a potent eosinophil chemokine and activating factor (8). Whether IL-13 directly contributes to esophageal tissue pathology (independent of eosinophils) has not been determined. While IL-13 has been shown to be involved in the development of tissue remodeling in the lung (9) and intestine (10), its role in the development of esophageal remodeling has not been examined. Experimental models of aeroallergen and IL-13 delivery to the lung has shown that eosinophils contribute to esophageal epithelial hyperplasia and collagen levels in the esophagus, at least in part. Yet, IL-13 has been shown to also induce tissue remodeling by eosinophil independent effects under a variety of conditions within multiple tissues(9–12).As such, it is now relevant to test whether IL-13 is capable of directly or indirectly inducing esophageal remodeling typical of EE and to determine the relevance of this process to human EE. In order to address this, we have utilized an inducible lung IL-13 transgenic murine model, wherein IL-13 is selectively overexpressed in the lungs in an externally regulated fashion following transgene induction with dietary doxycycline (DOX) (9). We aimed to determine the ability of chronic airway IL-13 stimulation to induce experimental EE with tissue remodeling, the mechanism and receptors involved in disease development, and the applicability of our results to human EE.

Methods & Materials

Inducible IL-13 lung transgenic mice

Bi-transgenic mice (CC10-iIL-13) were generated in which IL-13 was expressed in a lung-specific manner that allowed for external regulation of the transgene expression, as previously described(13). CC10-iIL-13 mice deficient in eosinophils, eotaxin-1, and eotaxin-2 were generated by breeding the CC10-iIL-13 (FVB/n) with the Δdbl-GATA (BALB/c), eotaxin-1 (SVEV), and eotaxin-2 (SVEV) gene-targeted mice for three generations. Δdbl-GATA mice were generously provided by Drs. Alison Humbles and Craig Gerard (Children's Hospital, Boston, MA). For all experiments, wild-type mice with the appropriate mixed backgrounds (FVB/N) were used as controls. Transgene expression was induced by feeding bi-transgenic mice Doxycycline-impregnated (DOX) food (625 mg/kg; Purina Mills, Richmond, IN). Animals were housed under specific pathogen-free conditions in accordance with institutional guidelines.

Quantification of tissue eosinophils

Esophageal eosinophils were detected using an immunohistochemical stain against murine eosinophilic major basic protein (MBP) as reported(9). Endogenous peroxidase activity was quenched using a 0.3% hydrogen peroxide in methanol solution. Tissue was then subjected to pepsin for 10 minutes at 37°C (DIGEST-ALLTM 3, Zymed Laboratories Inc.). Non-specific binding was blocked using 3% goat serum in PBS for 2 hours at room temperature followed by the addition of rabbit anti-murine MBP (1:8000) primary antibody (kindly provided by Dr. Jamie Lee, Mayo Clinic Scottsdale, AZ), which was allowed to incubate

overnight at 4°C. Slides were incubated with biotinylated goat anti-rabbit (1:250) secondary antibody for 40 minutes at room temperature and then incubated with an avidin-peroxidase complex for 30 minutes (Vector Laboratories). Development of peroxidase reaction was achieved by incubating slides with nickel diaminobenzidine-cobalt chloride solution (Vector Laboratories) for 4 minutes at room temperature and then counter-stained with nuclear fast red. Quantification of positive cells was performed using ImagePro Plus imaging software and results are reported as immunoreactive cells per square millimeter.

Epithelial thickness and collagen quantitation

Epithelial thickness was determined by staining cross-sectioned esophageal samples with H&E. Quantitation of thickness was performed using ImagePro Plus imaging software by taking 3–6 lengthwise measurements per slide from the lumen to the basement membrane of each esophagus. Collagen deposition was determined by staining esophageal samples with trichrome and quantitated using ImagePro Plus imaging software. Collagen measurements are recorded as area of collagen staining per length of basement membrane.

Analysis of epithelial cell proliferation

To determine the degree of epithelial cell proliferation, 5′-bromodeoxyuridine (BrdU) (Zymed Laboratories, San Francisco, CA) incorporation analysis was performed according to previously reported methods(6). In brief, DOX and NO-DOX mice were injected intraperitoneally with 0.25 ml of 5′-BrdU solution (0.75 μg BrdU) 2 hours before death. The esophagus was fixed with 10% neutral buffered formalin (Sigma) for 24 hours. After fixation, the tissue was embedded in paraffin, and 5 micron sections were processed using standard histologic approaches. Tissue was digested with trypsin (0.125%) for 3 minutes at 37°C, followed by incubation for 30 minutes at room temperature. Sections were washed with PBS 3 times for 2 minutes and further incubated with monoclonal biotinylated anti-BrdU antibody for 60 minutes at room temperature. Negative controls included replacing the primary antibody with PBS, and positive controls were provided by the manufacturer. Cells with nuclear staining for BrdU were detected with streptavidin-peroxidase and DAB substrate (Zymed Laboratories, San Francisco, CA), followed by counter staining with hematoxylin. The $BrdU^+$ cell quantitation was carried out with the assistance of digital morphometry as described above for eosinophils.

Assessment of angiogenesis

Tissues were fixed, embedded and sectioned and prepared as described above. Slides were trypsinized with 0.1% trypsin at 37°C for 5 min, (Difco) and incubated with 180 ml of methyl alcohol and 3 ml of 30% hydrogen peroxide, blocked with 2% rabbit serum/PBS/Triton for 2h, followed by incubation overnight with rat anti-mouse CD31 (PECAM-1) antibody (Pharmingen 01951D) at 4°C. Slides were then incubated with biotinylated rabbit anti-rat antibody (Vector Laboratory, BA-4001) for 30 min, developed with ABC complex and DAB substrate, and counter stained with 0.1% nuclear fast red in 5% aluminum sulfate for 2 min. Morphometry was used to determine the average number of PECAM-1 positive vessels per high power field in each group.

Determination of esophageal circumference

The esophagus was isolated by cutting the proximal end at the level of the cricoid ring and the distal end 2–5 mm above the stomach, then suspended in Hanks buffer and longitudinally exposed on an agarose gel for the measurement of esophageal circumference.

Measurement of IL-13 and IL-13/soluble IL-13Rα2 complex

Protein content of IL-13 and IL-13/soluble IL-13Rα2 complex was determined by ELISA(14). For IL-13, an IL-13-specific ELISA kit ((R&D Systems, Minneapolis, MN) was used to measure the protein level from homogenized tissue solutions. IL-13/IL-13Rα2 complex was quantified by using a capture ELISA method. Briefly, 96-well plates were coated with anti-IL-13 Ab (R&D Systems) overnight at 4°C. Samples of either blood serum or soluble extract of homogenized esophagus were applied to the plate and incubated at room temperature for 2 h. Wells were washed and then incubated with biotinylated anti-mouse IL-13Rα2 antibody (R&D Systems) for another 2 h. This was followed by streptavidin-HRP conjugate and substrate solution (R&D Systems) at room temperature for 20 min each. Absorbance was read at 450 nm, and OD readings were converted to nanograms per milliliter. To determine the total IL-13Rα2 level, samples were pre-saturated with IL-13 prior to be added to 96 wells. A saturation percentage was calculated using the ratio of IL −13/IL-13Rα2 complex divided by total /IL-13Rα2.

Microarray analysis

RNA from the esophagus or lung of IL-13 inducible transgenic mice obtained after 30 days of DOX or NO-DOX treatment was subjected to gene chip analysis using MOE 430 2.0 chips as previously reported (15). Gene transcript levels were determined using algorithms in the Microarray Analysis Suite and GeneSpring software (Silicon Genetics). For comparison with human EE, genes were translated to human homologues represented on the human U133 chip using GeneSpring software and compared to microarray results previously described(8, 15). Welch T test and fold change cut-off were performed. The correlation between IL-13 expression and numbers of dysregulated genes were also analyzed using GeneSpring software.

Real-time quantitative PCR analysis

RNA samples from the whole esophagus were subjected to reverse transcription analysis using SuperScript II reverse transcriptase (Invitrogen) according to manufacturer's instructions. Real-time PCR analysis of transgenic IL-13 and *rtTA* levels was performed using the LightCycler 480 system in conjunction with the ready-to-use LightCycler 480 SYBR Green I Master reaction kit (Roche Diagnostics). Results were normalized to *GAPDH* cDNA. Amplification of cDNA was achieved using the following primers: *transgenic IL-13* (205 bp), ATGGCTGGCAACTAGAAGGC and CATCTACAGGACCCAGAGGA; *rtTA* (200 bp), GCGCATTAGAGCTGCTTAATG and AAAATCTTGCCAGCTTTCCCC; Eotaxin 1 (87 bp), CCCAACACACTACTGAAGAGCTACAA and TTTGCCCAACCTGGTCTTG; Eotaxin 2 (280 bp), TGTGACCATCCCCTCATCTTGC and AAACCTCGGTGCTATTGCCACG; Human IL-13 (125 bp), ACAGCCCTCAGGGAGCTCAT and TCAGGTTGATGCTCCATACCAT.

Statistical analysis

Statistical significance comparing different sets of mice was determined by Student *t* test. *P* values <0.05 were considered statistically significant. SPSS software was used for the statistical analysis.

Results

Esophageal eosinophilia induced by the lung IL-13 transgene

Doxycycline (DOX) exposure of iIL-13 transgenic mice increased esophageal eosinophilia ~47-fold (Figure 1). Representative photomicrographs of untreated and DOX-treated mice

stained with anti-major basic protein (MBP) antibody to detect eosinophils are shown in Figure 1A and B, respectively. Eosinophils infiltrated all layers of the esophagus, including the muscularis mucosa, lamina propria and epithelium. A kinetic analysis revealed that esophageal eosinophilia peaked after 10 days of DOX and remained elevated during the 30-day experiment (Figure 1C). The kinetics of esophageal and pulmonary eosinophilia differed but both returned toward baseline level by 3 weeks after DOX withdrawal. Airway IL-13 did not increase eosinophil levels in gastrointestinal segments distal to the esophagus. For example, stomach eosinophil levels in untreated and DOX-treated mice were 12.4 ± 7.6/mm^2 and 14.1 ± 4.9/mm^2, respectively (p = 0.7).

Esophageal tissue remodeling induced by the lung IL-13 transgene

DOX ingestion for 30 days induced marked inflammatory and remodeling changes in the esophagus of iIL-13 transgenic mice (Figure 2). Microscopically, DOX increased epithelial thickness (Figure 2A–B and Supplemental Figure 1A) (this was also observed when tissue sections were stained with anti-MBP, trichrome, BrdU and anti-PECAM1, as shown in the Figure 1 and Figure 2C–H). Increased epithelial thickness was accompanied by increased epithelial cell proliferation, with an ~2-fold increase in epithelial layer $BrdU^+$ cell number, primarily associated with the basal zone (Figure 2C–D and Supplemental Figure 1B).

The effects of IL-13 on esophageal collagen and angiogenesis were also assessed. An increase in the area of collagen-stained material (detected mostly in the lamina propria in DOX-treated mice (Figure 2E–F)) was demonstrated by trichrome staining and morphometric analysis (Supplemental Figure 2A) (22 ± 7.3 vs. 43 ± 5.1 $m^2/\mu m$ basement membrane (mean ± S.D. n = 4; P < 0.01)). In addition, DOX treatment increased the intensity of trichrome staining (using 1–4+ scoring) from 1.3 ± 0.5 to 3.3 ± 0.5 (mean ± S.D, n = 4; P < 0.01). Staining with antibody to PECAM1, a vascular endothelial cell marker, revealed an increased number of blood vessels in DOX treated mice (Figure 2H) compared to control mice (Figure 2G). This was confirmed by morphometric analysis (Supplemental Figure 2B) and was mainly observed in the epithelial layer, just above the basement membrane regions.

Morphometric analysis also showed that the esophageal circumference was increased in DOX-treated mice (Figure 3A–B).

DOX treatment increases esophageal IL-13 protein, but not IL-13 mRNA

DOX treatment for 4 weeks increased IL-13 protein nearly 1000-fold in the lungs and ~8-fold in the esophagus of iIL-13 transgenic mice (Figure 4A). Esophageal IL-13 peaked after one week of DOX treatment, then reached a plateau over the next 3 weeks, while pulmonary IL-13 continued to increase. Transgenic IL-13 mRNA increased in the lung but not the esophagus during the same period (Figure 4B). DOX did not increase the expression of endogenous IL-13 mRNA (data not shown). The increased transgenic IL-13 mRNA in the lung but not in the esophagus is consistent with this lung specific IL-13 transgene model.

IL-13 induces marked in situ esophageal gene expression

To define the molecular pathways induced by IL-13 in the esophagus, we conducted a genome-wide microarray expression profile analysis of RNA isolated from the esophagus of IL-13 transgenic mice that were exposed to DOX for 30 days and compared the gene transcript levels to age- and gender-matched transgenic mice that were not exposed to DOX, using methods previously reported (9). DOX-induced IL-13 expression was associated with a significant difference in 767 genes ($p < 0.05$) in the esophagus of transgenic mice. This corresponds to 1.7% of the total transcriptome (45,101 genes). Among those 767 genes, 80 genes were modified ≥ 2 fold (Supplemental Table I). These genes encode cell signaling and

cellular adhesion proteins and cell surface glycoproteins. Eosinophil-associated ribonuclease, IL-1 receptor-like 1, mitogen activated protein kinase 1 (MAP4K-1), cholinergic receptor, leukotriene C4 synthase, complement component 3a receptor 1, and interferon-induced transmembrane protein 6 were included in the IL-13-induced EE transcriptome.

Comparison of human EE and IL-13-induced murine EE transcriptomes

There were 283 genes in the murine IL-13-induced esophageal transcriptome that overlapped with the human EE transcriptome ($P<0.05$) (Supplemental Table II). The genes significantly conserved between experimental EE and human EE are presented in a heat diagram (Figure 5 A). Functional analysis of genes that have >5-fold changes in either the human or murine system (Table I) revealed their involvement in cell communication, cytokine-cytokine receptor interaction, calcium signaling, histidine metabolism, complement and coagulation cascades, JAK-STAT signaling, and arachidonic acid metabolism. Notably, three CXC chemokines (CXCL1, 2 and 6) were also among those genes that overlapped. Both CXCL1 and CXCL2 have been shown to mediate IL-13 induced remodeling and inflammatory process in the lung (12, 16).

In the human system, 343 genes correlated with IL-13 mRNA levels (Figure 5 B and Supplemental Table III). These included known IL-13 induced genes such as eotaxin-3 as well as genes involved in tissue remodeling, such as collagen type VIII alpha2, cathepsin S, cathepsin C, and fibrinogen gamma chain. Taken together, these results suggest a role for IL-13 in esophageal remodeling in mouse and man.

IL-13 induces esophageal eotaxin-1 and eotaxin-2, which are required for esophageal eosinophilia

To investigate the mechanism of IL-13-induced eosinophilia in this experimental EE model, we examined eotaxin production in the lung and esophagus. Esophageal and lung protein levels of eotaxin-1 (Figure 6A) increased after 1 week of DOX administration and remain elevated after 4 weeks. The level of eotaxin-1 in the lung peaked by 4 weeks of DOX administration. The protein level of eotaxin-2 (Figure 6B) increased after 1 week of DOX administration and remained elevated at 4 weeks in the lung and esophagus. The level of eotaxin-1 and eotaxin-2 mRNA in the esophagus increased by 3.8 and 1.48-fold between no-DOX and DOX mice, respectively, using gene chip analysis. In order to investigate if eotaxin was mediating IL-13 driven esophageal eosinophilia, we generated IL-13 transgenic mice that were deficient in eotaxin-1 or eotaxin-2. These studies revealed that IL-13-driven esophageal eosinophilia was primarily eotaxin-1 dependent (Figure 6 C).

IL-13 induced esophageal remodeling is independent of eosinophils

To determine the role of eosinophils in promoting the tissue remodeling seen in the iIL-13 transgenic mice, we examined triple transgenic mice (CC10/IL-13/GATA-1 KO) that expressed iIL-13 but lack the eosinophil lineage because of deletion of the double palindromic site in the GATA1 promoter (ΔdblGATA). These triple transgenic mice had no esophageal eosinophila following DOX induction for 4 weeks (Figure 7 A), but still developed the same degree of tissue remodeling, including epithelial thickness (Figure 7 B), collagen deposition (Figure 7 C) and cellular hyperplasia (Figure 7 D). These data indicate that IL-13-induced esophageal tissue remodeling occurs independent of eosinophils in this animal model.

Increased accumulation of IL-13 receptors

To further investigate the mechanism of IL-13-induced EE, we examined the accumulation of IL-13Rα2 as well as IL-13/IL-13Rα2 protein complexes since IL-13Rα2 has been shown to have "decoy" effect on IL-13 function. Protein levels of free and IL-13-bound sIL-13Rα2 were increased in both the blood (Figure 8A) and the esophagus (Figure 8B) after 4 weeks of DOX. The data showed that essentially all of the sIL-13Rα2 is complexed with IL-13 in the esophagus, suggesting that free IL-13 may also be present. We also tested the mRNA expression of IL-13Rα2 using real time PCR. While DOX ingestion significantly increased pulmonary IL-13Rα2 expression ($P<0.05$), it had no significant effect on IL-13Rα2 expression in the esophagus ($P=0.15$) (data not shown).

Inhibitory effect of IL-13Rα2 on esophageal tissue remodeling in IL-13 lung transgenic mice

IL-13Rα2 has been described to be both an IL-13 antagonist and a mediator of IL-13-induced fibrosis (17, 18). To investigate the role of IL-13Rα2 in EE, we generated triple transgenic mice that overexpressed CC10/IL-13 and were genetically deficient in IL-13Rα2. DOX-induced IL-13 stimulated more severe esophageal remodeling in IL-13Rα2-deficient mice than in IL-13Rα2-sufficient mice (Fig 9).; there was increased epithelial thickness (Figure 9 B), collagen deposition (Figure 9 C) and esophageal circumference (Figure 9 D). Esophageal tissue eosinophilia, however, was similarly induced by IL-13 in IL-13Rα2-deficient and sufficient mice (Figure 9 A). The increased esophageal remodeling, lung inflammation and tissue necrosis induced by transgenic IL-13 in IL-13Rα2-deficient mice (not shown) was accompanied by increased weight loss and death (Figure 10).

Comparison of the IL-13-induced lung and esophageal transcriptomes

We aimed to define molecular pathways that would distinguish lung and esophageal responses induced by IL-13, especially since IL-13 induced remodeling is eosinophil-dependent in the lung (11) but not in the esophagus based on our current study. There were 836 genes modified by ≥2-fold in the lungs or esophagus. Cluster analysis stratified IL-13 induced genes into those conserved (clusters 2 and 4) and discordant (clusters 1 and 3) between the lungs and the esophagus (Figure 11). In cluster 2, 126 genes increased in both the lung and esophagus by > 5-fold (Supplemental Table IV). Notably, these gene families are involved in chemotaxis (C3a, CCL6, CCL8, CCL9, and CCL11), cytokine signaling (IL-27Ra, IL-7R and CSF receptors), and other immune and inflammatory functions (chitinase 3, platelet selectin, and serum amyloid). Consistent with a role for TGF-β and MMP-12 in promoting IL-13-induced esophageal fibrosis, DOX significantly increased levels of esophageal TGF-β_1 and MMP-12 mRNA by 2.0 and 2.7-fold, as assessed by gene chip analysis (data not shown). These two genes are increased in both the lung and esophagus (cluster 2 above). In cluster 4, 67 genes decreased in both the lung and esophagus by > 5-fold (Supplemental Table V). Among these genes were somatotropin hormone gene family (such as prolactin-like protein E), and ion binding protein genes (zinc finger protein 64 and carbonic anhydrase 3). Cluster 4 also included three genes involved in sensory perception (tectorin β, sry-box containing gene and cadherin 23) and two genes involved in neurogenesis (zinc finger protein of the cerebellum 2 and paired box gene 5). Other genes in this cluster included IL-12β, adrenergic receptor α 2c, and keratin complex 2. In cluster 3, 52 genes decreased in the lung but increased in the esophagus (Supplemental Table VI). In cluster 1, 39 genes increased in the lung but decreased in the esophagus (Supplemental Table VII). Clusters 1 and 3 are particularly interesting since these transcriptomes may be associated with tissue specific function. Taken together, these results indicate that IL-13 induces a set of shared and tissue specific genes in the lung and esophagus.

Discussion

Esophageal eosinophilia is the characteristic finding of human EE but the mechanisms involved in tissue pathology, including the role of eosinophils, remain poorly understood (19). Among environmental factors, both food and aeroallergen hypersensitivity have been implicated in the induction of EE, suggesting the involvement of Th2 immunity. Indeed, the Th2 cytokine IL-13 has been shown to be markedly overexpressed in the esophagus of EE patients and to induce eotaxin-3 in esophageal epithelial cells, yet the involvement of IL-13 with other aspects of disease remains uncertain. In this study, inducible expression of IL-13 in the lung resulted in extensive esophageal eosinophilia and tissue remodeling. While lung eosinophilia was also observed, the kinetics of eosinophilia was different between the lung and esophagus. In fact, esophageal eosinophilia peaked around day 10 following DOX induction, which is earlier than the peak of lung eosinophilia post DOX induction. Interestingly, both lung and esophageal eosinophilia returned to near baseline level three to four weeks following withdrawal of DOX, suggesting that the IL-13 induced eosinophilia is reversible, similar to its reversibility following therapy in patients.

In asthma patients, tissue remodeling has an important role in chronic inflammation and is part of the mechanism of airway obstruction (20). In EE patients, esophageal remodeling including increased tissue fibrosis and angiogenesis occurs even in pediatric patients (3); however, the mechanisms that promote these changes remain unclear. Our study establishes that over-expressing lung IL-13 induces extensive esophageal tissue remodeling including increased epithelial thickness, collagen deposition, epithelial cell proliferation, angiogenesis and esophageal circumference. The increased esophageal circumference, which is visible to the naked eye, may be responsible for the esophageal furrowing notable by endoscopic analysis in patients (21). Following IL-13 lung transgene induction, a significant accumulation of IL-13 protein was observed in both the lung and the esophagus. The content of IL-13 in the lung was much higher than that in the esophagus, consistent with the lung specific IL-13 transgene design. In addition to the accumulation of IL-13 protein, both IL-13/IL-13Rα2 complex and total IL-13Rα2 were increased following iIL-13 transgene induction. The increased IL-13Rα2 level in the blood and esophagus may be explained by the increased IL-13Rα2 mRNA expression in the lung and the complex of sIL-13/IL-13Rα2 may serve as a transport system for IL-13 to be delivered to the esophagus. Consistent with this model, IL-13 mRNA in situ hybridization failed to detect IL-13 positive cells in the esophagus of the IL-13 expressing mice (data not shown). Alternatively, IL-13 protein accumulation in the esophagus may be derived from swallowing lung-derived IL-13. Free IL-13 that is produced in the lung and swallowed or that goes from lung to blood to the esophagus likely binds to the type 2 IL-4R in the esophagus. The lack of gastric and intestinal eosinophilia distal to the esophagus is more compatible with a swallowing theory. Regardless, tissue eosinophilia did not occur distal to the esophagus, highlighting that esophageal tissue specific effect of IL-13, at least in this experimental system.

In this study, we observed the co-existence of esophageal eosinophilia and tissue remodeling. Moreover, we demonstrate that eotaxin-1 (but not eotaxin-2) is required for esophageal eosinophilia. Notably, murine eotaxin-3 is a pseudogene in mice, and mouse eotaxin-1 appears to be the functional homologue of human eotaxin-3, which is the main chemokine operational in human EE (22, 23). Furthermore, we demonstrate that esophageal remodeling is eosinophil-independent, inasmuch as we observed the same degree of tissue remodeling in eosinophil-sufficient and –deficient IL-13 transgenic mice. As such, we have identified an IL-13-driven pathway that mediates EE-like changes independent of eosinophils, suggesting that some aspects of the disease may occur independent of eosinophils in humans. In our prior studies, we have demonstrated a role of IL-5 driven eosinophils in aeroallergen-induced epithelial proliferation (as measured by BrdU and basal

layer thickness) and collagen layer thickness (5). As such, the present study is the first to identify eosinophil-independent responses in EE. Preliminary studies in humans have suggested that humanized anti-IL-5 is a potentially useful therapy for lowering esophageal eosinophilia although an effect on remodeling has not yet been proven; in fact, the limited patients examined still have extensive tissue remodeling (22, 24). We recognize that our system involves supraphysiological levels of IL-13, so the direct action of IL-13 (not requiring eosinophils) may not apply to an antigen-driven process in patients. Nevertheless, our study provides a rationale for therapeutic intervention focused on the non-eosinophil components of the disease. Furthermore, since IL-13 induced lung remodeling (using the same transgenic system) is eosinophil dependent (11); whereas, the remodeling in the esophagus was not, our study highlights distinct pathways for disease induction between the lung and esophagus even when disease is driven by the same atopic trigger (in this case IL-13). Indeed, transcript expression profile analysis readily identified shared and unique molecular events between the lung and esophagus.

To further explore the mechanisms of IL-13-mediated tissue remodeling, we utilized a triple transgenic CC10/IL-13 /IL-13Rα2 deletion mouse model. The triple transgenic mice with IL-13Rα2 deletion showed significantly enhanced remodeling including increased esophageal mucosal thickening and collagen deposition as well as clinical features (weight loss and death) compared to the double transgenic mice. The observed enhanced esophageal remodeling following IL-13Rα2 deletion indicates that IL-13Rα2 inhibits IL-13 induced remodeling, consistent with a “decoy” effect of IL-13Rα2 that prevents IL-13 binding to the stimulatory type 2 IL-4R (17, 25) and recent results with IL-13 transgenic IL-13Ra2 deficient mice in the lung (26). These findings indicate that IL-13Rα2-mediated TGF-β-dependent fibrotic effect (27) are not likely operational in EE.

Taken together, our study establishes that: (1) pulmonary IL-13 expression induces extensive esophageal tissue eosinophilia and remodeling, including fibrosis, angiogenesis, and epithelial hyperplasia; (2) IL-13 promotes increased esophageal circumference; (3) esophageal eosinophilia is mediated by eotaxin-1 (and not eotaxin-2); (4) tissue remodeling occurs largely independent of eosinophils; (5) IL-13Rα2 dampens IL-13 mediated esophageal pathology and clinical features; (6) IL-13 induces a marked esophageal transcriptome in vivo in mice that overlaps with the human EE transcriptome, at least in part; and (7) IL-13-induces a set of shared gene in the lung and esophagus. Additional translational studies demonstrate that IL-13 levels directly correlates with relevant gene expression in esophageal tissue from EE patients. As such, we establish that IL-13 is sufficient to induce significant esophageal pathology and remodeling in vivo, that this process is likely operational in human EE, and we identify that disease pathology of EE occurs largely independent of eosinophils (under these experimental conditions) and is inhibited by IL-13Rα2. Consequently, pharmacological targeting of IL-13 production and signaling may be a worthwhile pursuit.

Supplementary Material

Refer to Web version on PubMed Central for supplementary material.

Acknowledgments

The authors would like to thank Drs. Simon Hogan, Anil Mishra, Amal Assa’ad, Margaret Collins, Eric Brandt, and Nives Zimmermann for their advice and technical assistance. We are also grateful for the help of CCHMC Pulmonary and Pathology Morphology Core laboratories. We thank Dr. James Lee from Mayo Clinic for providing anti-MBP reagent, and Dr. Jeffrey Whitsett (Cincinnati Children’s Hospital Medical Center) for kindly providing the CC10 activator mice.

This work was supported in part by the R01 AI42242, RO1 AI45898, RO1 DK076893, P01 HL076383, P30 DK 0789392, T32 AI 060515, T32 DK 07727-12 and the kind support of the CURED, Buckeye and Food Allergy Project Foundations, as well as AAAAI and Food Allergy Initiative Award.

Reference

1. Furuta GT, Liacouras CA, Collins MH, Gupta SK, Justinich C, Putnam PE, Bonis P, Hassall E, Straumann A, Rothenberg ME. Eosinophilic esophagitis in children and adults: a systematic review and consensus recommendations for diagnosis and treatment. Gastroenterology. 2007; 133:1342–1363. [PubMed: 17919504]
2. Zuo L, Rothenberg ME. Gastrointestinal eosinophilia. Immunol Allergy Clin North Am. 2007; 27:443–455. [PubMed: 17868858]
3. Aceves SS, Newbury RO, Dohil R, Bastian JF, Broide DH. Esophageal remodeling in pediatric eosinophilic esophagitis. J Allergy Clin Immunol. 2007; 119:206–212. [PubMed: 17208603]
4. Spergel J, Rothenberg ME, Fogg M. Eliminating eosinophilic esophagitis. Clin Immunol. 2005; 115:131–132. [PubMed: 15885634]
5. Mishra A, Hogan SP, Brandt EB, Rothenberg ME. An etiological role for aeroallergens and eosinophils in experimental esophagitis. J. Clin. Invest. 2001; 107:83–90. [PubMed: 11134183]
6. Mishra A, Rothenberg ME. Intratracheal IL-13 induces eosinophilic esophagitis by an IL-5, eotaxin-1, and STAT6-dependent mechanism. Gastroenterology. 2003; 125:1419–1427. [PubMed: 14598258]
7. Akei HS, Mishra A, Blanchard C, Rothenberg ME. Epicutaneous antigen exposure primes for experimental eosinophilic esophagitis in mice. Gastroenterology. 2005; 129:985–994. [PubMed: 16143136]
8. Blanchard C, Mingler MK, Vicario M, Abonia JP, Wu YY, Lu TX, Collins MH, Putnam PE, Wells SI, Rothenberg ME. IL-13 involvement in eosinophilic esophagitis: transcriptome analysis and reversibility with glucocorticoids. J Allergy Clin Immunol. 2007; 120:1292–1300. [PubMed: 18073124]
9. Fulkerson PC, Fischetti CA, Hassman LM, Nikolaidis NM, Rothenberg ME. Persistent effects induced by IL-13 in the lung. Am J Respir Cell Mol Biol. 2006; 35:337–346. [PubMed: 16645178]
10. Fichtner-Feigl S, Fuss IJ, Young CA, Watanabe T, Geissler EK, Schlitt HJ, Kitani A, Strober W. Induction of IL-13 triggers TGF-beta1-dependent tissue fibrosis in chronic 2,4,6-trinitrobenzene sulfonic acid colitis. J Immunol. 2007; 178:5859–5870. [PubMed: 17442970]
11. Fulkerson PC, Fischetti CA, Rothenberg ME. Eosinophils and CCR3 regulate interleukin-13 transgene-induced pulmonary remodeling. Am J Pathol. 2006; 169:2117–2126. [PubMed: 17148674]
12. Lee PJ, Zhang X, Shan P, Ma B, Lee CG, Homer RJ, Zhu Z, Rincon M, Mossman BT, Elias JA. ERK1/2 mitogen-activated protein kinase selectively mediates IL-13-induced lung inflammation and remodeling in vivo. The Journal of clinical investigation. 2006; 116:163–173. [PubMed: 16374521]
13. Wan H, Kaestner KH, Ang SL, Ikegami M, Finkelman FD, Stahlman MT, Fulkerson PC, Rothenberg ME, Whitsett JA. Foxa2 regulates alveolarization and goblet cell hyperplasia. Development. 2004; 131:953–964. [PubMed: 14757645]
14. Khodoun M, Lewis CC, Yang JQ, Orekov T, Potter C, Wynn T, Mentink-Kane M, Hershey GK, Wills-Karp M, Finkelman FD. Differences in expression, affinity, and function of soluble (s)IL-4Ralpha and sIL-13Ralpha2 suggest opposite effects on allergic responses. J Immunol. 2007; 179:6429–6438. [PubMed: 17982031]
15. Blanchard C, Wang N, Stringer KF, Mishra A, Fulkerson PC, Abonia JP, Jameson SC, Kirby C, Konikoff MR, Collins MH, Cohen MB, Akers R, Hogan SP, Assa'ad AH, Putnam PE, Aronow BJ, Rothenberg ME. Eotaxin-3 and a uniquely conserved gene-expression profile in eosinophilic esophagitis. The Journal of clinical investigation. 2006; 116:536–547. [PubMed: 16453027]
16. Cho SJ, Kang MJ, Homer RJ, Kang HR, Zhang X, Lee PJ, Elias JA, Lee CG. Role of early growth response-1 (Egr-1) in interleukin-13-induced inflammation and remodeling. J Biol Chem. 2006; 281:8161–8168. [PubMed: 16439363]

17. Mentink-Kane MM, Wynn TA. Opposing roles for IL-13 and IL-13 receptor alpha 2 in health and disease. Immunol Rev. 2004; 202:191–202. [PubMed: 15546394]

18. Fichtner-Feigl S, Strober W, Kawakami K, Puri RK, Kitani A. IL-13 signaling through the IL-13alpha2 receptor is involved in induction of TGF-beta1 production and fibrosis. Nat Med. 2006; 12:99–106. [PubMed: 16327802]

19. Rothenberg ME. Eosinophilic gastrointestinal disorders (EGID). J Allergy Clin Immunol. 2004; 113:11–28. [PubMed: 14713902]

20. Ward C, Johns DP, Bish R, Pais M, Reid DW, Ingram C, Feltis B, Walters EH. Reduced airway distensibility, fixed airflow limitation, and airway wall remodeling in asthma. Am J Respir Crit Care Med. 2001; 164:1718–1721. [PubMed: 11719315]

21. Nurko S, Teitelbaum JE, Husain K, Buonomo C, Fox VL, Antonioli D, Fortunato C, Badizadegan K, Furuta GT. Association of Schatzki ring with eosinophilic esophagitis in children. J Pediatr Gastroenterol Nutr. 2004; 38:436–441. [PubMed: 15085025]

22. Bullock JZ, Villanueva JM, Blanchard C, Filipovich AH, Putnam PE, Collins MH, Risma KA, Akers RM, Kirby CL, Buckmeier BK, Assa'ad AH, Hogan SP, Rothenberg ME. Interplay of adaptive th2 immunity with eotaxin-3/c-C chemokine receptor 3 in eosinophilic esophagitis. J Pediatr Gastroenterol Nutr. 2007; 45:22–31. [PubMed: 17592361]

23. Borchers MT, Ansay T, DeSalle R, Daugherty BL, Shen H, Metzger M, Lee NA, Lee JJ. In vitro assessment of chemokine receptor-ligand interactions mediating mouse eosinophil migration. J Leukoc Biol. 2002; 71:1033–1041. [PubMed: 12050190]

24. Stein ML, Collins MH, Villanueva JM, Kushner JP, Putnam PE, Buckmeier BK, Filipovich AH, Assa'ad AH, Rothenberg ME. Anti-IL-5 (mepolizumab) therapy for eosinophilic esophagitis. J Allergy Clin Immunol. 2006; 118:1312–1319. [PubMed: 17157662]

25. Morimoto M, Zhao A, Sun R, Stiltz J, Madden KB, Mentink-Kane M, Ramalingam T, Wynn TA, Urban JF Jr, Shea-Donohue T. IL-13 Receptor {alpha}2 Regulates the Immune and Functional Response to Nippostrongylus brasiliensis Infection. J Immunol. 2009

26. Zheng T, Liu W, Oh SY, Zhu Z, Hu B, Homer RJ, Cohn L, Grusby MJ, Elias JA. IL-13 receptor alpha2 selectively inhibits IL-13-induced responses in the murine lung. J Immunol. 2008; 180:522–529. [PubMed: 18097054]

27. Fichtner-Feigl S, Young CA, Kitani A, Geissler EK, Schlitt HJ, Strober W. IL-13 signaling via IL-13R alpha2 induces major downstream fibrogenic factors mediating fibrosis in chronic TNBS colitis. Gastroenterology. 2008; 135:2003–2013. 2013 e2001–2007. [PubMed: 18938165]

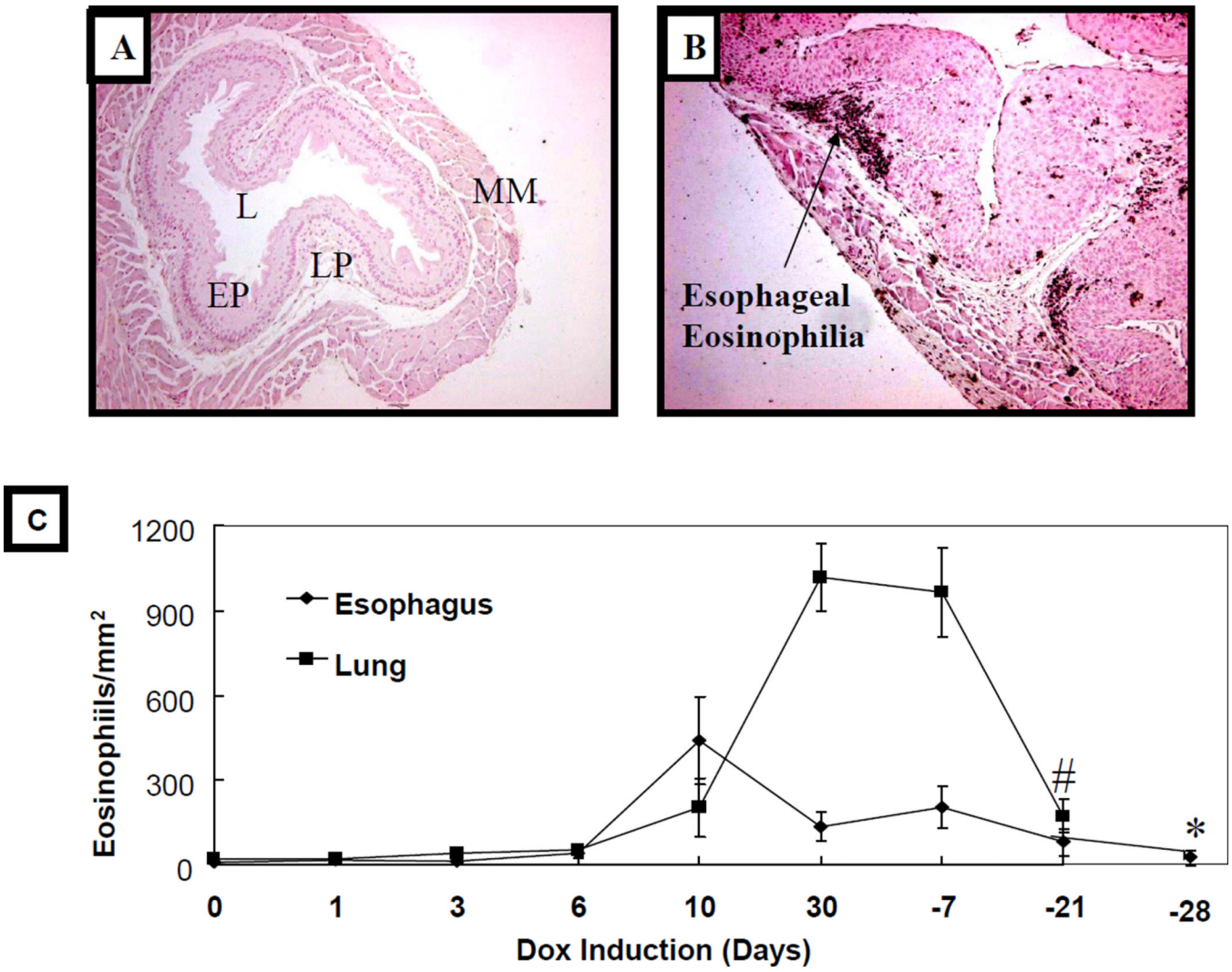

Figure 1. IL-13 transgene inducible esophageal eosinophilia

The esophagus of IL-13 lung transgenic mice before (A) and after (B) 4 weeks of DOX exposure was stained with anti-MBP to identify eosinophils. Eosinophils are identifiable by dark immunostaining. LP, lamina propria; L, lumen; EP, epithelial; and MM, muscularis mucosa. The kinetics of eosinophilia in the lung and esophagus of IL-13 lung transgenic mice is shown in (C). Data are representative of three independent experiments with $n = 6$ mice per time point in each experiment. Original magnification for both A&B, X100.

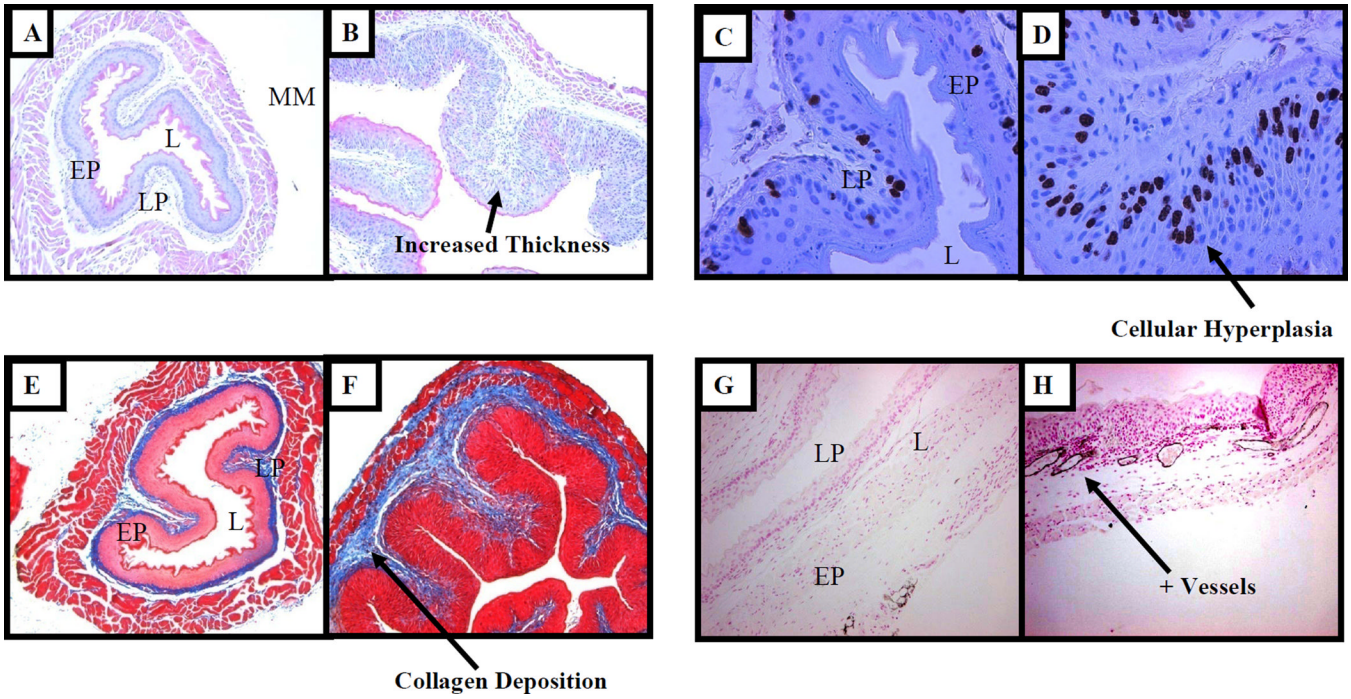

Figure 2. IL-13 transgene inducible esophageal tissue remodeling

The esophagus of IL-13 lung transgenic mice before (NO-DOX) (A, C, E, G) and after (B, D, F, H) 4 weeks of DOX exposure was stained with H&E (A, B), for BrdU incorporation (C, D), trichrome (E, F) and anti-PECAM-1 (G, H). Representative images are shown of three independent experiments with $n = 6$ mice in each experiment. Original magnification for A&B, E&F and G&H, X100; for C&D, X400

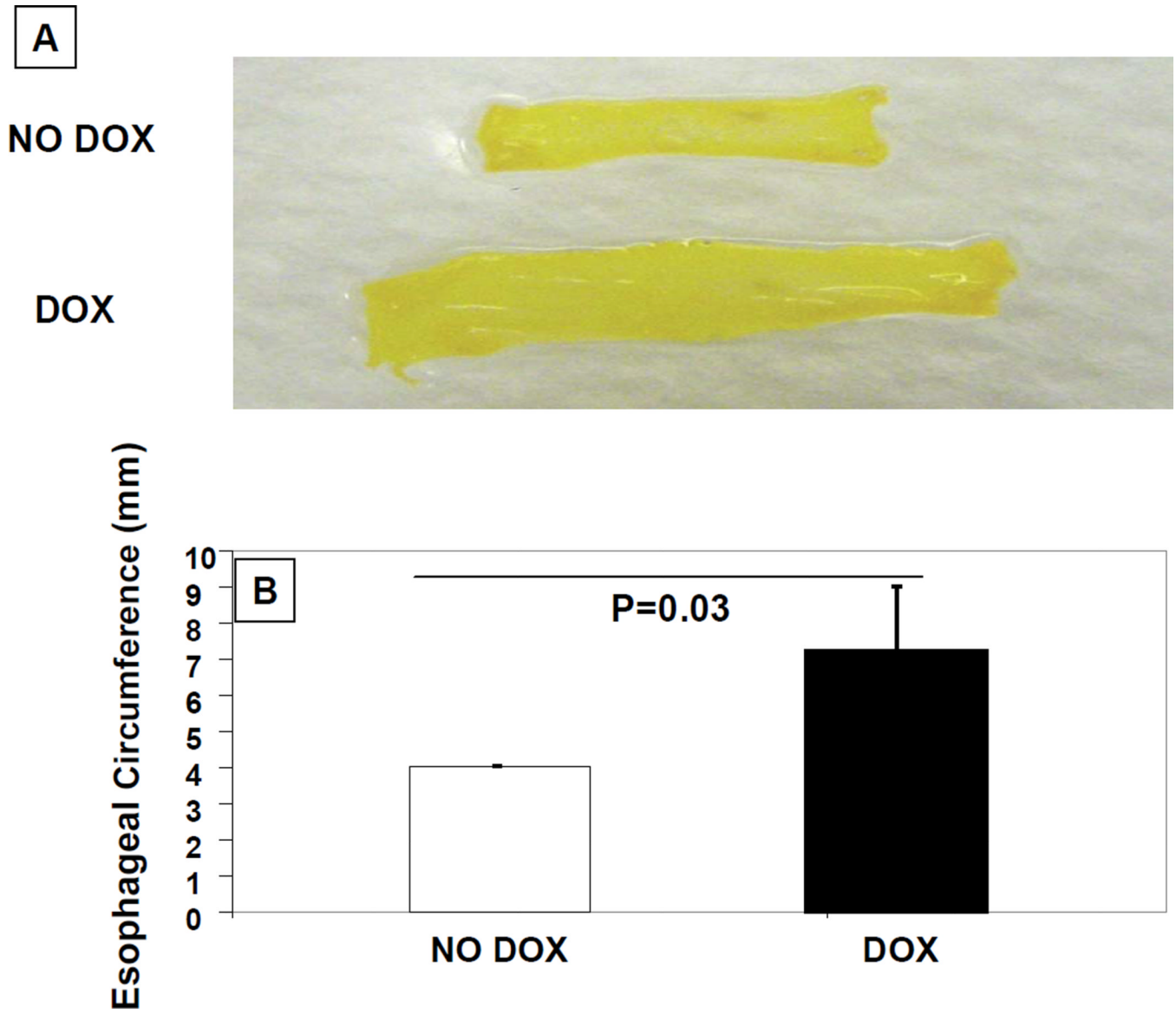

Figure 3. Esophageal circumference

The excised esophagus before (NO DOX) and after DOX exposure is shown in (A). Quantitative assessment of the esophageal circumference is shown in (B). The results are presented as Mean ± SD, n = 6 mice and the experiment were repeated independently at least three times.

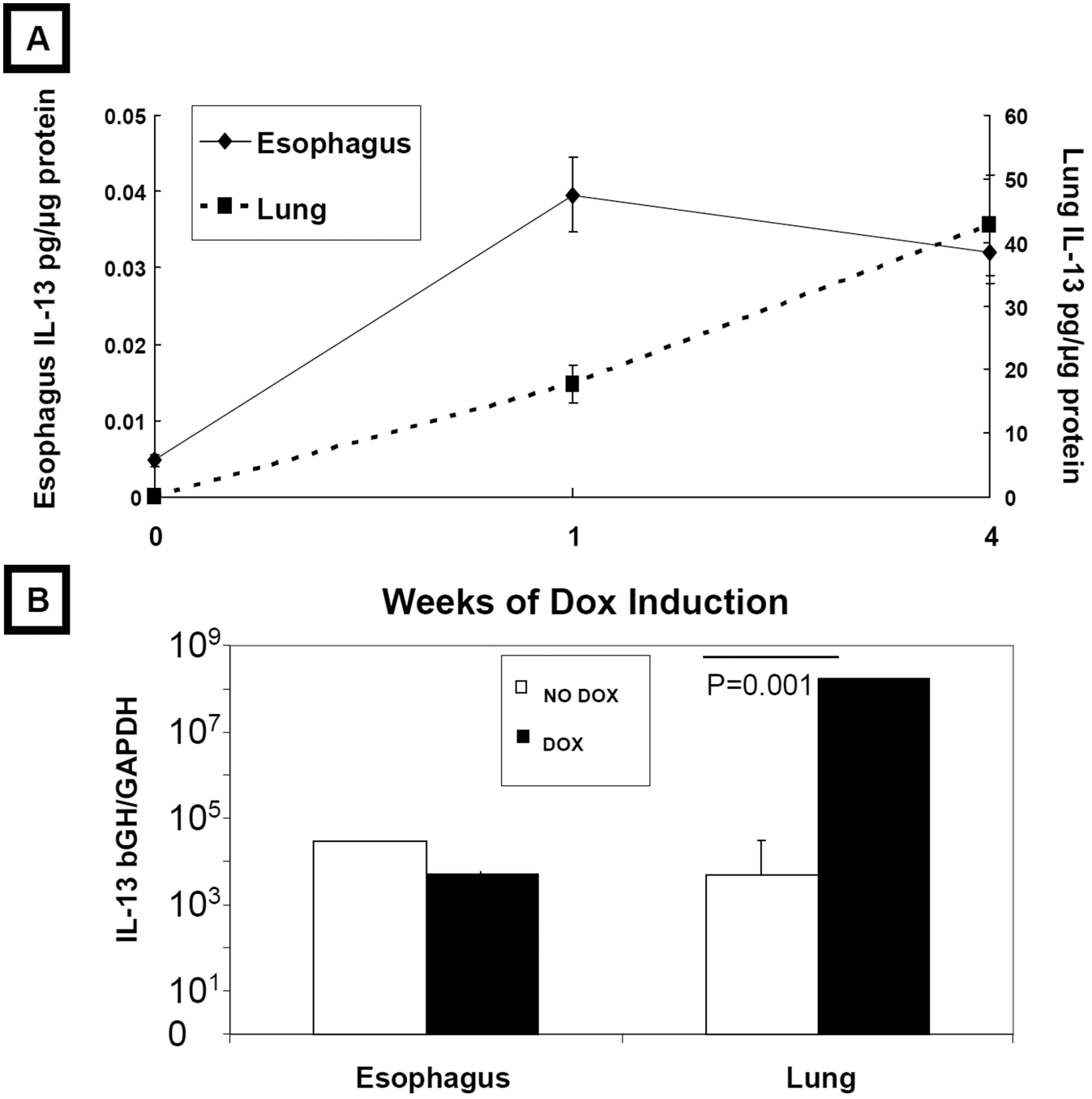

Figure 4. IL-13 accumulation and expression in the esophagus and lung

(A) Protein levels of IL-13 from lung and esophageal tissue (n = 8 mice for each group) following a time course of DOX exposure were measured by ELISA. (B) The expression of IL-13 mRNA in the esophagus and lung following 4 weeks of DOX vs. NO-DOX exposure is shown. Real-time PCR analysis of IL-13 expression level is performed and results are normalized to *GAPDH* cDNA. The results are the summary of three independent experiments, reported as mean ± SD with n = 6 mice for each group or time point in each experiment.

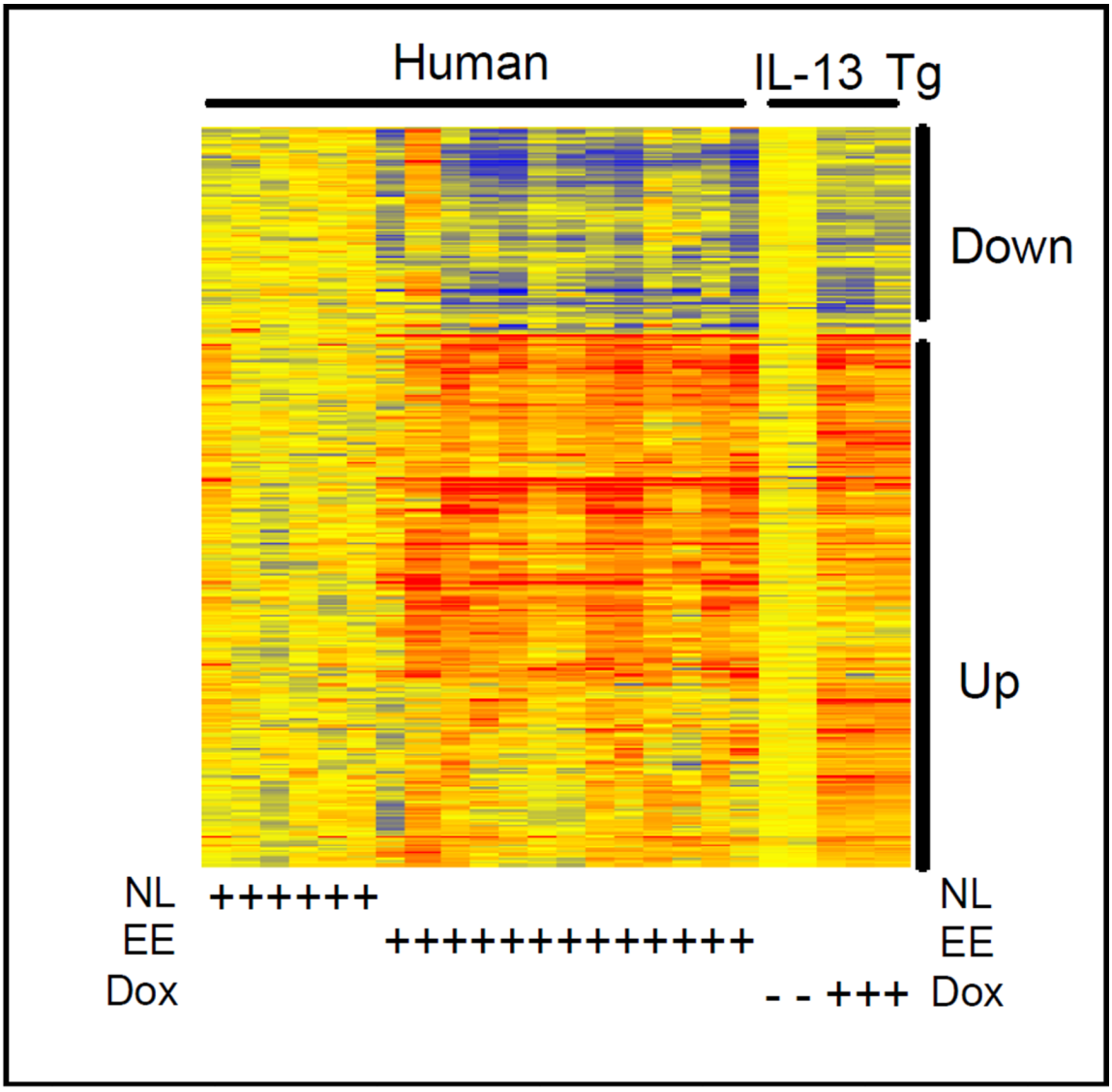

A.

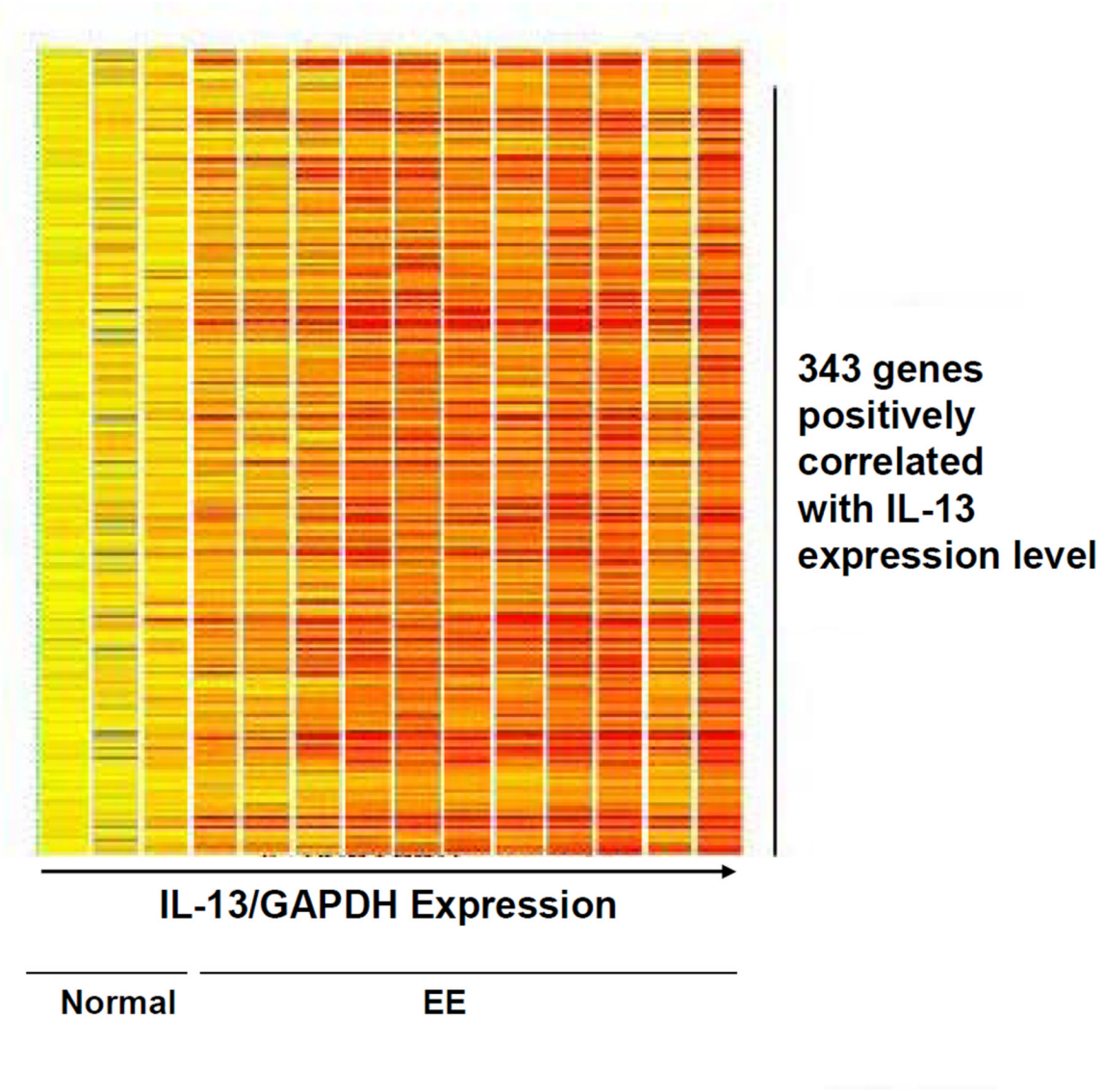

B.

Figure 5. A. Esophageal transcript profile of lung specific IL-13 transgenic mice
Microarray analysis of the lung and esophagus in DEX-treated CC10-rtta tet/on-IL13 transgenic mice, and comparison with the human EE esophagus. Cluster tree analysis of IL-13 transgenic esophagus and human EE. The 283 genes presented in the heat diagram (standard correlation) correspond to genes significantly different in experimental EE ($p<0.01$) and human EE ($p<0.01$) compared to their respective controls (NO-DOX and normal (NL) patient esophageal biopsies, respectively. Each line represents a separate individual. Upregulated and downregulated genes are shown in red and blue, respectively. **B. The correlation between IL-13 expression and dysregulated genes.** The 343 genes correlated with eosinophil levels (based on Spearman correlation) are shown in the gene tree format. Samples are organized in the order of increased IL-13 expression (from left to right) with each sample normalized for GAPDH expression. Samples with a level below detection

limit (not detectable) are presented in the group ND. This data represents samples from a single patient but it was repeatable in different patient samples.

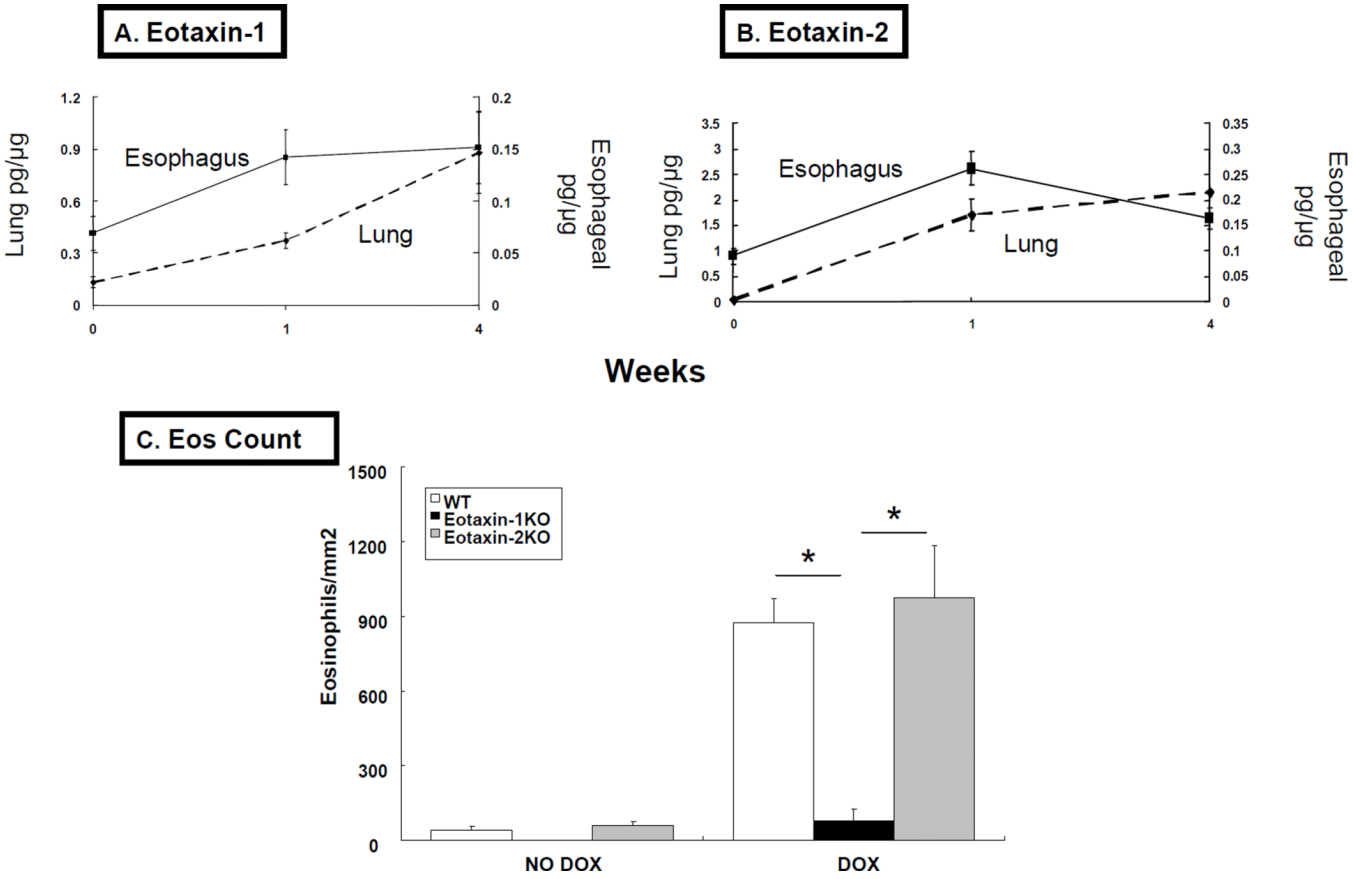

Figure 6. Eotaxin production in the lung and esophagus

Protein levels of eotaxin 1 (A) and eotaxin-2 (B) in the esophagus are shown after 1-4 weeks of DOX administration. Results were normalized to the esophageal protein content and are expressed as mean ± SD; * = P <0.01 comparing to Dox on week 0. The esophageal eosinophil count from IL-13 transgenic mice was compared with IL-13/Eotaxin-1 and 2 KO mice (C). * = P<0.001 WT vs. KO. The figures are the summary of three independent experiments. n= 4 for each group per experiment.

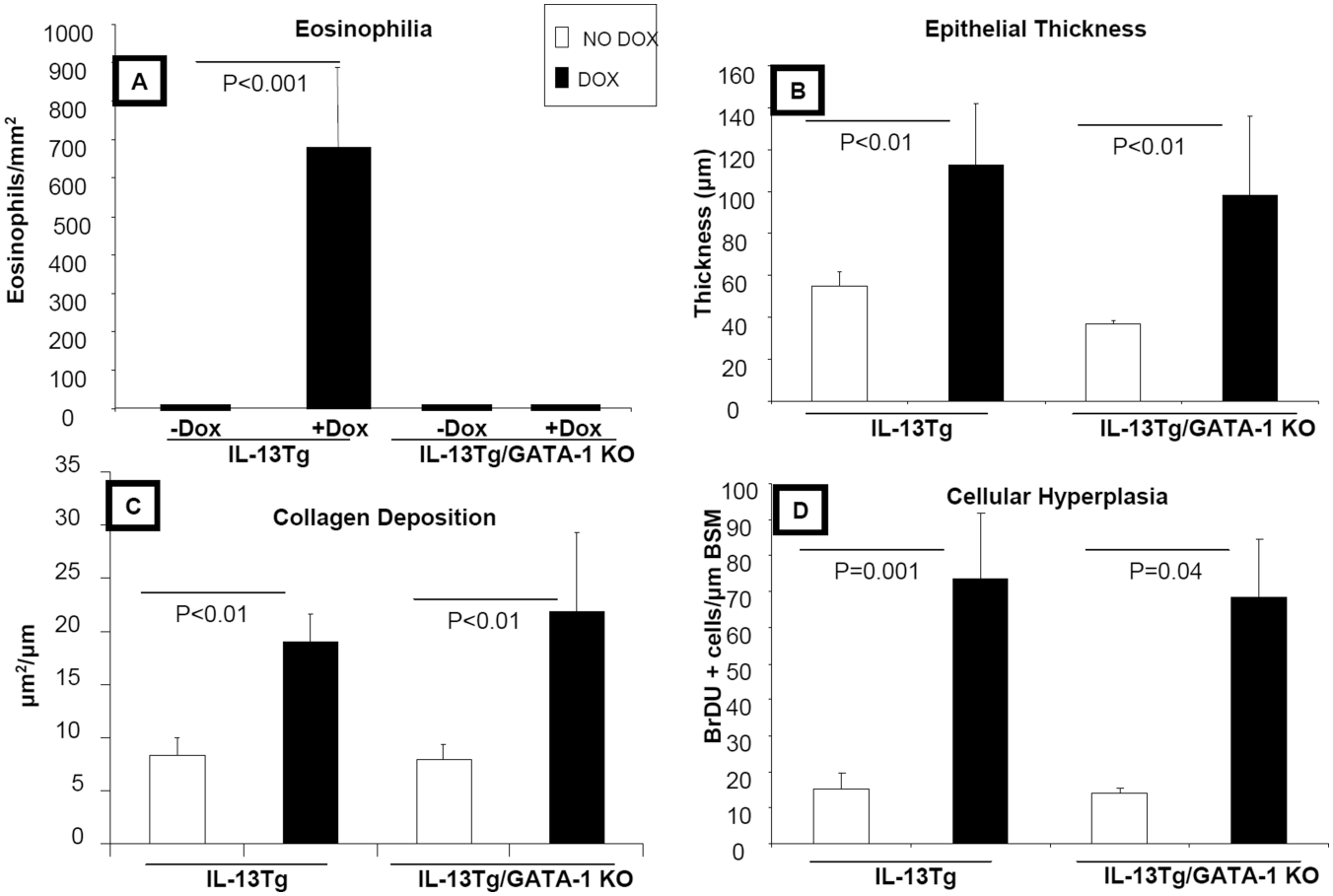

Figure 7. Effect of Δdbl-GATA (GATA-1 KO) on IL-13 transgene inducible esophageal tissue remodeling

The esophagi of IL-13 lung transgenic mice and IL-13 tg- GATA-1 KO after 4 weeks of DOX exposure were stained with anti-MBP (A), H&E (B), trichrome staining (C) and BrDU (D). Morphometric analysis was shown for each of those measurements. The figures are the summary of three independent experiments. n= 4 for each group per experiment.

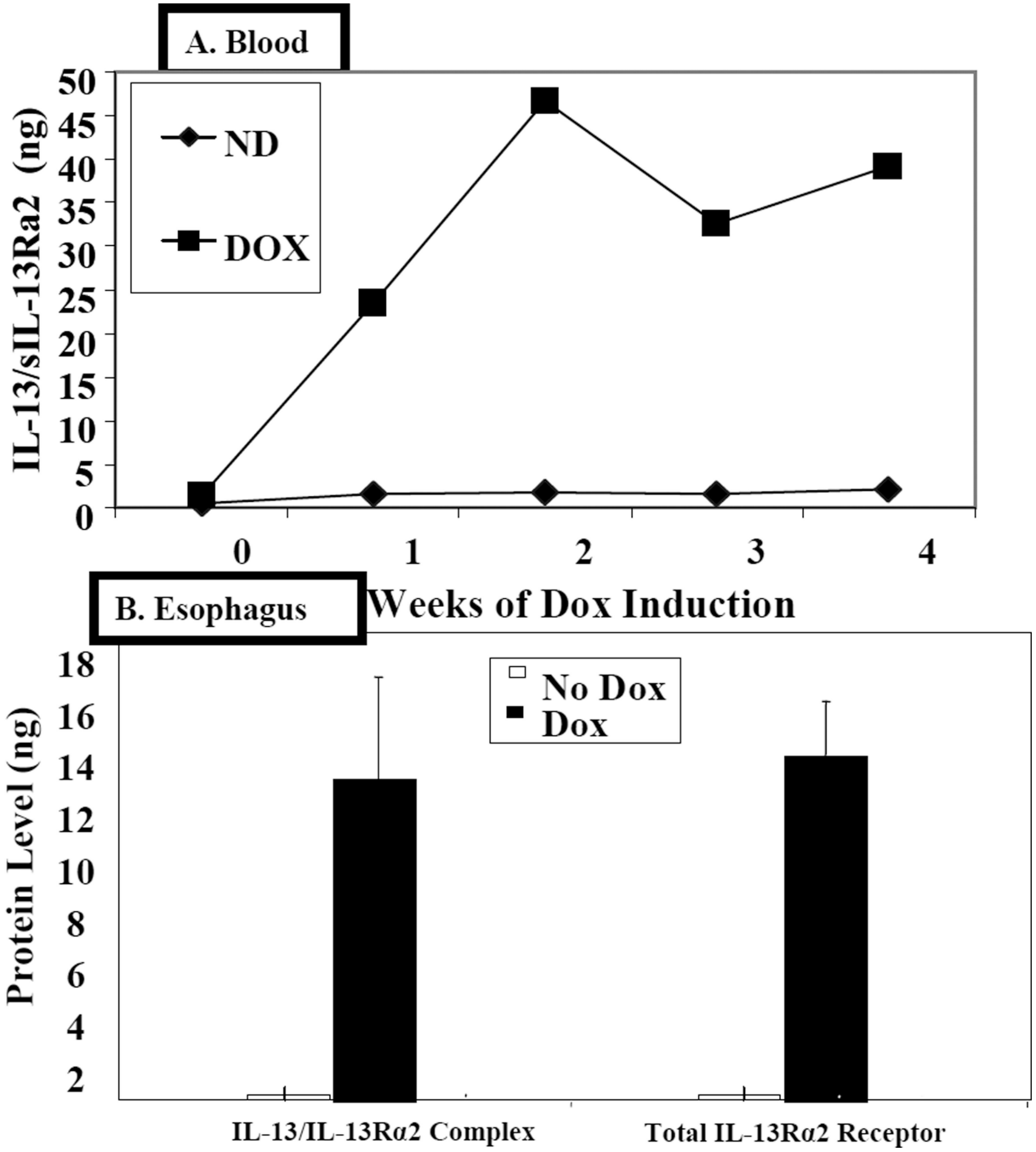

Figure 8. Accumulation of IL-13/sIL-13Rα2 complexes

Protein levels of blood IL-13/sIL-13Ra2 complex (A) following a time course of DOX exposure were measured using ELISA. Protein content of esophageal IL-13/sIL 13Ra2 complex and total sIL-13Ra2 after 4 weeks of DOX exposure were also measured by the same method (B). The figures are the summary of three independent experiments. n= 4 for each group per experiment.

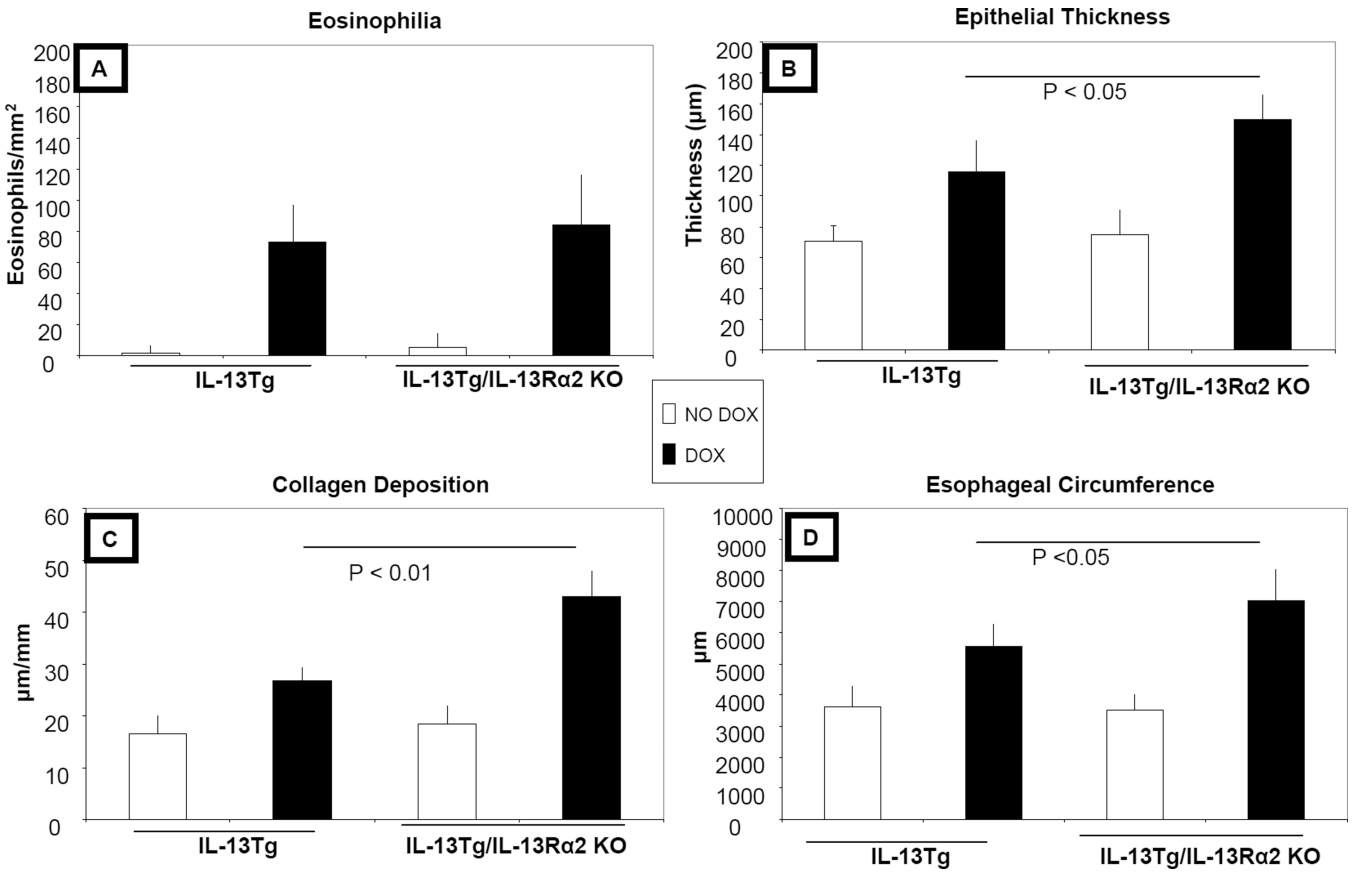

Figure 9. Effect of IL-13Rα2 deficiency on IL-13 transgene-inducible esophageal tissue remodeling

The esophagus of IL-13 lung transgenic mice with or without IL-13Rα2 deletion were studied for esophageal eosinophilia (A), epithelial thickness (B), collagen deposition (C) and esophageal circumference (D). The figures are the summary of three independent experiments. n= 4 for each group per experiment.

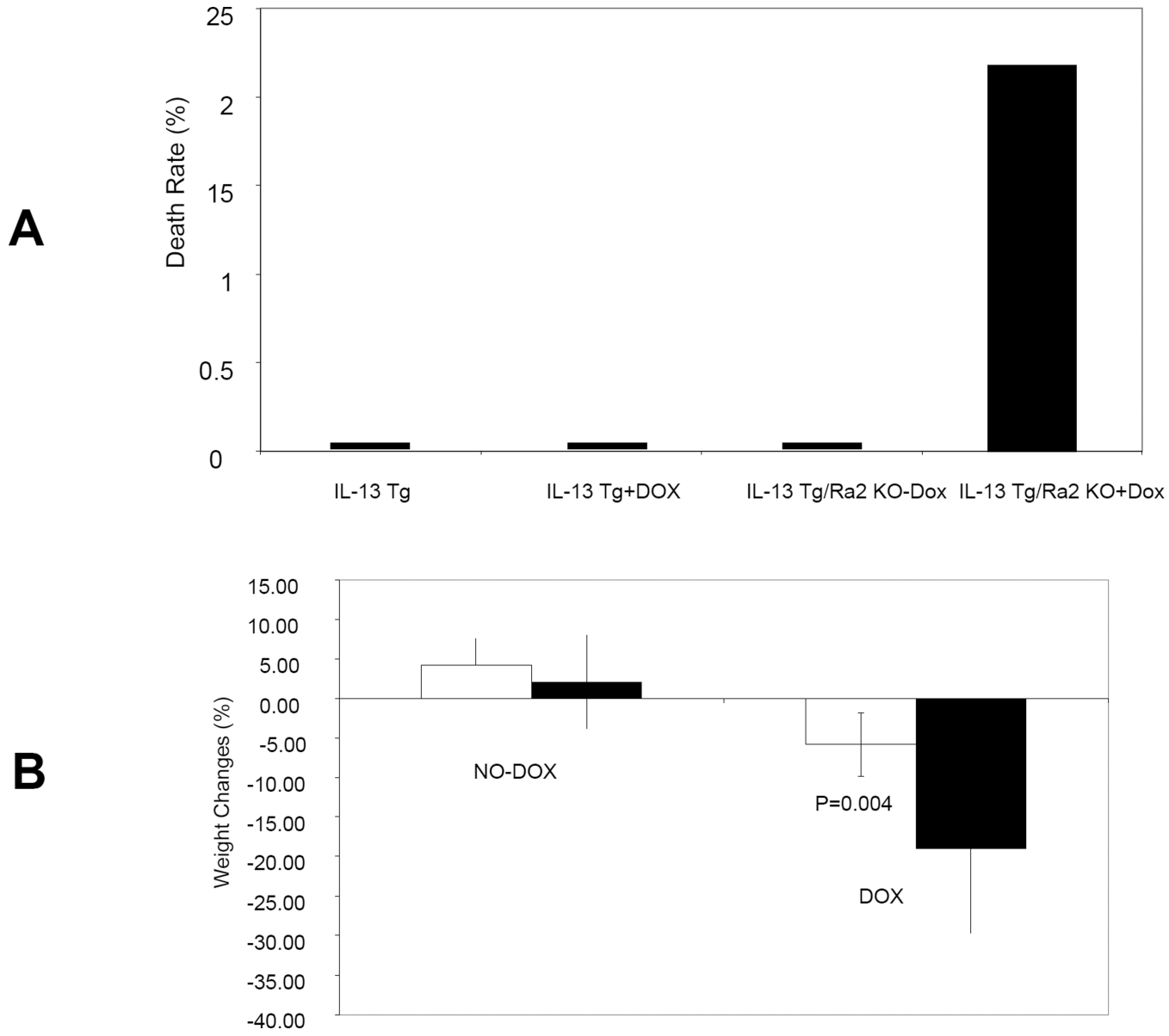

Figure 10. Effect of IL-13Ra2 deficiency on death rate and weight loss

The death rate (A) and weight loss from IL-13 transgenic mice with or without IL-13Rα2 deficiency, after 4 weeks of DOX exposure, were shown. The figures are the summary of three independent experiments. n= 4 for each group per experiment.

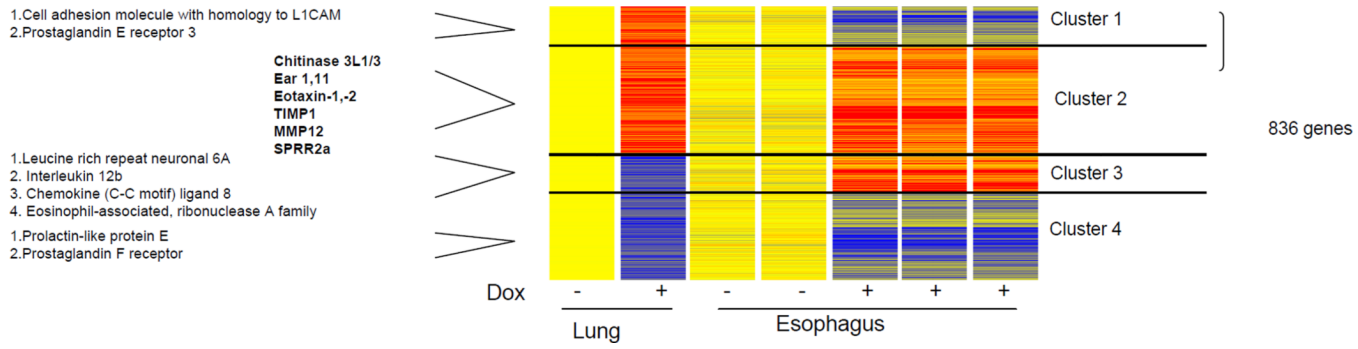

Figure 11. Esophageal transcript profile of lung specific IL-13 transgenic mice

Comparison of transcript profiles of CC10-rtta tet/on- IL-13 transgenic mice in the lungs and esophagus. The genes (2-fold cut-off) in lungs of mice treated with doxycycline (DOX, 30 days) or left untreated (NO-DOX) was compared to the genes significantly different ($p < 0.01$) in the esophagus of mice treated with DOX (30 days) or left untreated (NO-DOX). The overlap of the two signatures, composed of 836 genes, is presented in a heat diagram and is clustered using gene tree analysis (standard correlation). Cluster 1 contains genes upregulated (red) in the lung and down regulated (blue) in the esophagus. Cluster 2 contains genes upregulated in the lung and the esophagus. Cluster 3 contains genes down regulated in the lung and upregulated in the esophagus. Cluster 4 contains genes down-regulated in the lung and the esophagus.

Table I

Comparison of human EE and IL-13-induced murine EE transcriptomes

Functional analysis of genes that have >5-fold changes in either the human or murine system revealed their involvement in cell communication, cytokine-cytokine receptor interaction, calcium signaling, histidine metabolism, complement and coagulation cascades, JAK-STAT signaling, and arachidonic acid metabolism. Those genes are among genes in the murine IL-13-induced esophageal transcriptome that overlapped with the human EE transcriptome (P<0.05). ND, No Dox; Dox, Dox for 4 weeks; NL, biopsy samples from non-EE patients; EE, biopsy samples from EE patients.

Affy #	ND vs Dox	NL vs EE	Symbol	Gene name
207328 at	78.97	21.27	ALOX15	Arachidonate 15-lipoxygenase
204470 at	21.58	17.41	CXCL1	Chemokine (C-X-C motif) ligand 1
206336 at	3.526	9.173	CXCL6	Chemokine (C-X-C motif) ligand 6
206529_x_at	6.125	8.25	SLC26A4	Solute carrier family 26, member 4
204580 at	42.84	7.781	MMP12	Matrix metalloproteinase 12
207134_x_at	1.313	7.732	TPSB2	Tryptase beta 2
209301 at	4.088	6.847	CA2	Carbonic anhydrase II
203854 at	3.346	6.522	IF	I factor (complement)
205579 at	4.06	5.666	HRH1	Histamine receptor H1
206172 at	5.426	5.12	IL13RA2	Interleukin 13 receptor, alpha 2
205681 at	6.3	3.246	BCL2A1	BCL2-related protein A1
207067 s at	5.76	3.141	HDC	Histidine decarboxylase
206134 at	5.073	2.853	ADAMDEC1	ADAM-like, decysin 1
223502 s at	7.902	2.073	TNFSF13B	Tumor necrosis factor superfamily, member 13b
209875_s_at	9.593	1.795	SPP1	Secreted phosphoprotein 1
205965 at	10.18	1.456	BATF	Basic leucine zipper transcription factor, ATF-like
209800 at	20.56	1.282	KRT16	Keratin 16
221698_s_at	5.522	1.257	CLEC7A	C-type lectin domain family 7, member A
209774_x_at	7.863	1.197	CXCL2	Chemokine (C-X-C motif) ligand 2
233534_at	0.188	0.187	KRTAP3-2	Keratin associated protein 3-2